ANALYSIS AND MODELING OF COMBINED DISCHARGE THROUGH BOX CULVERTS AND OVER CONTRACTED BROAD-CRESTED WEIRS

Abdel-Azim M. Negm

Associate Professor, Dept. of Water & Water Structures Eng.,
Faculty of Engineering, Zagazig University, Zagazig, Egypt
E-mail: amnegm85@yahoo.com

ABSTRACT

An experimental investigation is conducted on simultaneous flow through culvert and over broad-crested weir. The flow at the culvert outlet is considered as submerged flow. Both the culvert and the broad-crested weir (BCW) widths are smaller than the channel width. The characteristics of the simultaneous flow through both structures and the effects of flow and geometrical parameters of the structure were presented in the first part of this paper. In this part, discharge prediction models are developed using (a) multiple linear regression, (b) basic discharge equations of BCW and culvert and (c) artificial neural networks. The prediction and performance of each of the three models are compared using four criteria, namely, (i) mean relative absolute error, MRAE, (ii) root mean square error RMSE, (iii) coefficient of correlation, R, and standard error of estimate, SEE. Analysis of results indicated that the ANNs are powerful prediction tool compared to other models followed by the model based on the basic discharge equations of BCW and culvert. Sensitivity analysis is also conducted to reflect the relative importance of the involved variables.

Keywords: Broad-crested weirs, Culvert, Prediction models, Simultaneous flow, Hydraulic structures, Artificial neural networks

1. INTRODUCTION

Both culverts and broad-crested weirs are used for flow rate measurements in open channels as a separate structure. When existing culvert becomes inadequate to carry the required discharge due one reason or another, one of two alternatives are common, a replacement by a new culvert of larger capacity or capacity improvement by installing another one adjacent to the old. A third alternative may be proposed by employing a broad-crested weir over the culvert deck by constructing the weir walls above the culvert body and elevating the roadway above the weir through a bridge. Figure 1 shows a definition sketch for this alternative to illustrate the involved variables in the present paper. The third Alternative was investigated by Mohamed [1] and Negm [2] from the hydraulics point of view. A short review of the related studies to each structure separately was introduced by Mohamed [1] and Negm [2].

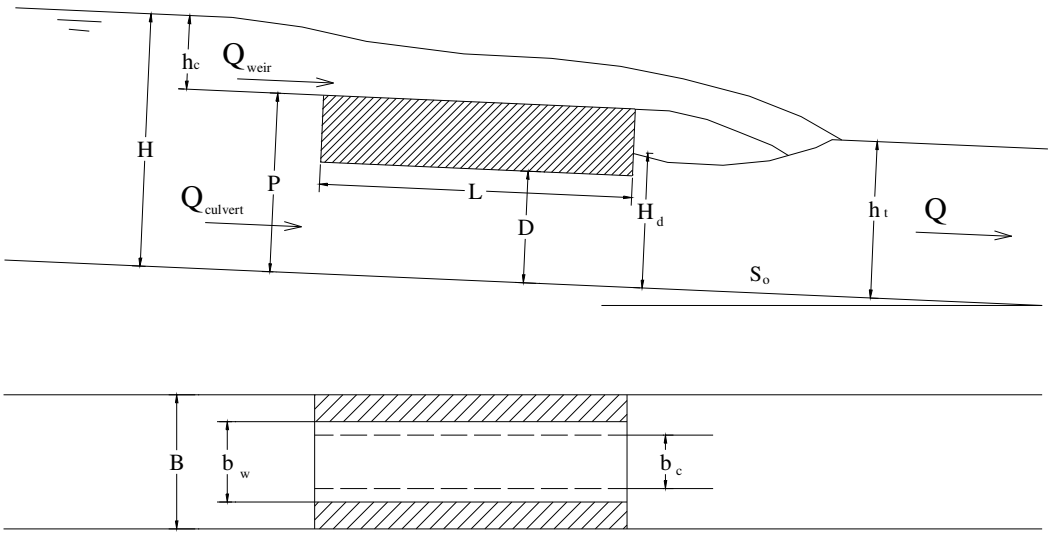

Figure 1. Definition sketch for simultaneous flow through box culvert and over contracted broad crested weir.

Flow through culverts is controlled by many variables including the inlet geometry, roughness, size, slope, approach and tailwater conditions. Exact determination of type of flow through culvert needs laboratory or field investigations. Generally speaking, culverts may be flowing full or partly full. They flowing full when both the inlet and the outlet are submerged or when the inlet is submerged and the outlet is not but the culvert is long enough to be considered as hydraulically long, Chow [3]. Variety of flow types could take place through culverts. The criteria controlling each type of flow and the corresponding discharge equation could be found in e.g. Herschy [4] and French [5]. For more detailed information on different types of flow though culverts, Manning roughness coefficients and discharge coefficients for culvert, interested reader can consult Bodhaine [6].

On the other hand, broad-crested weir (BCW) is a simple measurement device with the advantage of easy construction, easy installation and structure stability. The specification of broad-crested weirs and installation procedures for accurate measurements can be found in e.g. Bos [7]. A review of the studies concerning free and submerged flow characteristics over suppressed BCW was presented in Negm and Alshaikh [8]

Recently, an experimental investigation was conducted by Mohamed [1] to study the characteristics of simultaneous flow over contracted BCWs and through box culverts. The effects of submergence S, relative width of weir b_w/D, and relative width of culvert b_c/D, on the combined dimensionless discharge $Q/D^2\sqrt{2gD}$ (with D being the height of the culvert vent, b_c is the width of culvert vent, Q is the combined discharge and g is the gravitational acceleration). The following regression model (R^2 = 0.973 and SEE = 0.177) was provided to estimate the discharge through the combined structure having a bottom slope equals 0.006.

$$Q/D^2\sqrt{2gD} = -0.074 - 1.059S + 0.225\left(\frac{H}{D}\right)^2 + 1.33\frac{b_w}{D} + 0.819\frac{b_c}{D} - 2.329\frac{b_w}{b_c} \qquad (1)$$

Which is valid within the following limitations: $3 \le S \le 4$, $1.4 \le b_w/D \le 3$, $1.67 \le b_c/D \le 3$, $0.53 \le b_w/b_c \le 1.286$ and $S_o=0.006$.

Mohamed's work was extended by Negm [2] to investigate the effects of slope and both flow and geometrical parameters of the simultaneous flow. All the collected data due to both studies of Mohamed [1] and Negm [2] was used to develop a general prediction model instead of Eq.(1) to include the effect of bottom slope along with the other parameters as follows ($R^2 = 0.973$ and SEE=0.174):

$$Q/D^2\sqrt{2gD} = -0.708 - 1.082S + 0.24\left(\frac{H}{D}\right)^2 + 1.33\frac{b_w}{D} + 0.817\frac{b_c}{D} - 2.334\frac{b_w}{b_c} + 63.75S_o \qquad (2)$$

Which is valid within the following limitations: $3 \le S \le 4$, $1.4 \le b_w/D \le 3$, $1.67 \le b_c/D \le 3$, $0.53 \le b_w/b_c \le 1.286$ and $0.006 \le S_o \le 0.011$.

In this paper, discharge prediction models are developed using two different approaches. The first is by utilizing the basic equations of culvert and BCW and the second by applying the artificial neural networks. Results of both models are compared to those of equations 1 and 2.

2. THEORETICAL ANALYSIS

The simultaneous discharge shown by Figure 1 could be obtained by summing up the discharge over the broad-crested weir and that passing through the culvert. The discharge over the broad-crested weir can be computed from the following equation, Bos [7] and Negm and Alshaikh [8]

$$Q_w = \frac{2}{3}C_d C_v b_w \sqrt{\frac{2}{3}g}h_w^{3/2} \qquad (3)$$

In which Q_w is the discharge over the weir, C_d is the coefficient of the discharge of the weir, C_v is the coefficient of velocity, $C_v=(H_o/h_w)^{1.5}$, H_o is the total energy head over the weir, $H_o=h_w+V^2_a/2g$, V_a is the velocity of approach, $V_a= Q/(BH)$, Q is the total incoming discharge, B is the width of the approaching channel, H is the depth of flow in the approaching channel, b_w is the width of weir, g is the gravitational acceleration and h_w is the head of water over the weir.

On the other hand, the discharge passes through the culvert $h_t/D>1.0$ and $H/D>1.0$ is given by the following equation, French [5]

$$Q_c = C_D A_o \left[\frac{2g(H-h_t)}{1+\left(29C_D^2 n^2 L/R_o^{4/3}\right)}\right]^{1/2} \qquad (4)$$

In which Q_c is the discharge through the culvert, A_o is the cross sectional area of the culvert, R_o is the hydraulic radius of the culvert, C_D is the discharge coefficient of the

culvert, n is the Manning roughness coefficient of the culvert materials, L is the length of the culvert, h_t is the tailwater depth downstream the culvert.

The simultaneous discharge over the weir and through the culvert could be obtained by adding equation 4 to equation 3:

$$Q = F\left(\frac{2}{3}C_d C_v b_w \sqrt{\left(\frac{2}{3}\right)g}h_w^{3/2} + C_D A_o\left[\frac{2g(H-h_t)}{1+\left(29C_D^2 n^2 L/R_o^{4/3}\right)}\right]^{1/2}\right) \quad (5)$$

In which F is a factor to account for the interaction between the flow over the weir and that through the culvert. The interaction factor F is to be determined experimentally or from field data whenever available.

3. EXPERIMENTAL ARRANGEMENT

The experimental work of the present paper was conducted by Mohamed [1] and Negm [2] in a horizontal rectangular flume 30.5 cm wide, 31 cm high and 9.5 m long.. The flume is equipped with a tail gate to control the tailwater depth. A centrifugal pump lifts water from underground sump to the flume inlet. Water runs through the flume then returns back to the sump tank via a measuring tank. The collected experimental data are used in this paper to calibrate equation 5 and to train the developed artificial neural network model.

A typical tested model consisted of a contracted broad-crested weir combined with one vent box culvert with the same total length from entrance to exit of 40 cm. Also, the height of the culvert barrel was kept constant to 6 cm. Nine data sets (143 runs) was collected by Mohamed [1] while only four sets (77 runs) were carried out by Negm [2] as indicated by Table 1. During the course of the experimental programs, the flow at both inlet and outlet of the culvert were submerged and the culvert is flowing full. Also, the approaching discharge to the structure was more than the capacity of the culvert and thus a flow over the weir was expected. The recorded measurements include the flow depth at 40 cm upstream from the culvert inlet and just downstream of the culvert to ensure that the flow over the weir is free. The tailwater depth was recorded several times for each discharge to account for the effect of submergence. The discharge was measured by a pre-calibrated V-notch installed in a measuring tank located below the flume outlet at its downstream end and is connected directly to underground sump tank. Water depths were measured using a precise point gauge (up to ± 0.1 mm accuracy) mounted on instrument carriage.

Table 1 Experimental conditions of the collected data

Series	b_c	S	b_w/D	b_c/D	b_w/b_c	S_o	Source
A	12.0	3.33-4.0	3.0	2.0	1.286	0.006	Ref. [1]
B	14.0	3.33-4.0	3.0	2.3	1.286	0.006	Ref. [1]
C	18.0	3.00	1.8-2.6	3.0	0.6-0.87	0.006	Ref. [1]
D	18.0	3.67	1.8-3.0	3.0	0.6-1.0	0.006	Ref. [1]
E	18.0	4.00	1.8-3.0	3.0	0.6-1.0	0.006	Ref. [1]
F	10.0	3.00	1.4	1.67-3.0	0.53-0.84	0.006	Ref. [1]
G	10.0-18.0	3.33	1.4	1.67-3.0	0.53-0.84	0.006	Ref. [1]
H	10.0	3.67	1.4	1.67-3.0	0.53-0.84	0.006	Ref. [1]
I	10.0-18.0	4.00	1.4	1.67-3.0	0.53-0.84	0.006	Ref. [1]
TA	18.0	3.0-4.5	3.0	3.0	1.0	0.011	Ref. [2]
TB	18.0	3.0-4.0	3.0	3.0	1.0	0.003	Ref. [2]
TC	12.0-18.0	3.00	3.0	2.0-3.0	1.0-1.5	0.006	Ref. [2]
TD	18.0	3.33	1.8-3.0	3.0	0.6-1.0	0.006	Ref. [2]

4. CALIBRATION OF THE PROPOSED MODEL

The discharge through the combined structure could be computed using equation (5). If the following factors are well defined:

4.1. MANNING ROUGHNESS COEFFICIENT OF THE CULVERT MATERIALS N.

Since all the tested models in this paper are made from smooth and clean prespex, the Manning roughness coefficient is assumed to be 0.01.

4.2. THE DISCHARGE COEFFICIENT OF THE CULVERT, C_D

For this particular type of flow through culvert, the discharge coefficient of the box culvert with wing walls and the square top entrance is not beveled is taken as 0.75, French [5].

4.3. THE COEFFICIENT OF VELOCITY OF THE WEIR C_V

Since each of the weir width and the culvert width is less than the channel width, the approaching channel is wide enough such that the approach velocity is very small and hence the coefficient of velocity could be neglected. However, the total energy is computed and the average coefficient of velocity for the weir is found to be 1.000135. This means that considering the energy head will increase the flow due to the weir by an amount of about 0.0135%. Therefore, the coefficient of velocity is assumed unity in this work.

4.4. THE DISCHARGE COEFFICIENT OF THE WEIR C_d

The values of h_w/L is almost less than 0.4 while $h_w/(h_w+P)$ is almost less than 0.45. In this case a correction factor of 1.025 is applied to the basic discharge coefficient of the broad-crested weir which is equal to C_d=0.848. However, the use of the basic discharge coefficient of 0.848 is accurate enough because the use of the correction factor does not improve the performance of the equation significantly. When using the basic coefficient of discharge, the values of R^2 and RMSE are 0.9887 and 0.432 respectively while they are 0.9885 and 0.434 when a correction factor is applied. Therefore, C_d is assumed to be 0.848.

4.5. THE INTERACTION FACTOR F

The simultaneous discharge is computed using equation 5. Under the assumption F=1. The value of F is then computed by dividing the actual measured discharge by the computed discharge. Several approaches were employed in order to select a proper value of F. The best approach was to correlate the interaction factor F to the factors of equation 2 which govern the simultaneous discharge as it improves the performance of the prediction model (equation 5). The obtained regression equation for F is as follows (R^2=0.954 and SEE=0.0287)

$$F = 1.375 - 0.0376S - 0.0675\left(\frac{H}{D}\right) + 0.0124\frac{b_w}{D} + 0.0953\frac{b_c}{D} - 0.3815\frac{b_w}{b_c} + 16.265S_o \quad (6)$$

5. VERIFICATION OF THE MODEL (EQUATION 5)

Equation 5 with F as defined by equation 6 is used to compute the simultaneous discharge over the weir and through the culvert. Also, equations 1 and 2 are used to do the same. The computed values are compared to the measured simultaneous discharge. The comparisons are displayed in terms of the mean relative absolute error MRAE, the root mean square error RMSE, the correlation coefficient R, and the standard error of estimate SEE. The results are shown in table 2.

Table 2 Comparison between measurements and predictions of equations 1, 2 and 5

Criterion	Eq. 1.	Eq. 2.	Eq. 5, F= Eq. 6.	ANN
MRAE%	4.220	3.868	2.264	0.009
RMSE	0.839	0.670	0.432	0.170
R	0.979	0.986	0.994	0.999
SEE	0.177	0.174	0.431	0.170
Residuals, R	0.082	0.002	0.016	0.013
Max. +ve error	16.88	18.72	8.13	6.29
Max. –ve error	0.0	-11.54	-11.6	-3.79
% Obs. with error <5%	63.6	73.2	91.3	98.18 (<2.5%)

Also, Figure 2 presents the comparison between the measurements and the prediction of equation (5) with F defined by equation 6. Clearly, from Table 1 and Figure 2, equation (5) performs satisfactory well compared to other developed regression models because equation (5) has the lowest vales of MRAE, RMSE and SEE and the highest value of R compared to equations (1) and (2).

6. BUILDING THE ARTIFICIAL NEURAL NETWORKS MODEL

Artificial neural networks or simply neural networks are a new way of analyzing data. They have a unique ability to learn complex patterns and trends in the data emulating the human ability to solve complicated problems. Therefore, neural computing are based on the way that biological system, such as human brain, work. The human brain is made up of many neurons. Each of the brain cells is connected to many others in a network that adopts and changes as the brain learns. In neural computing, processing elements (PE) replace the neurons and these PEs are linked together to form neural networks. Each PE performs a simple task. It is the connections between the PEs that give neural networks the ability to learn patterns and interrelationship in data through the certain weights associated to the connections PEs. Early works on using ANN in the field of hydraulics were published during the last decade, e.g. Grubert [9], Dibike and Abbott [10] and Dibike et al. [11].

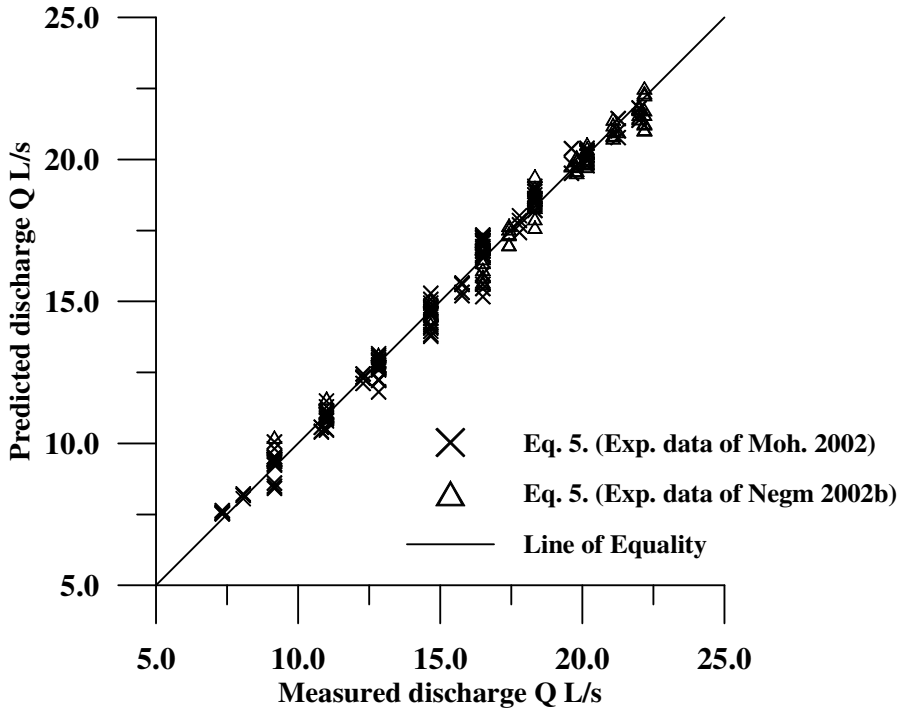

Figure 2. Prediction of equation (5) with F as given by equation 6 versus measured data due to Mohamed [1] and Negm [2]

The most important tool of ANN applied in this study is the multi-layer perceptrons (MLP) which is a neural network modeling tool that is optimized for prediction and forecasting applications, Neural Connection [12]. The MLP can be used to classify patterns or to predict values from data. The MLP learns from examples by providing the data to the neural network through an input tool or input layer which consists of a number of PEs equals the number of input variables or fields such that each PE represents one variable or one filed. These data are processed in a second layer called hidden layer because of all the processing and computations through this core layer are hidden from the users. More than one hidden layer could be used depending of the complexity of the application (if no hidden layer is used, it is a simple perceptron).The processed data are sent to the output layer that consists of a number of PEs equals to the number of targets (or number of desired outputs) in the application. All the PEs or neurons of each layer are connected the PEs of the preceding and following layers by links or connections without feedbak (therefore they are MLP foreword networks) but not to other neurons within the layer. A typical network of this type for the present application consisted of three layers as shown in Figure 3. Input layer of 6 neurons (or 6 PEs) to represent the dimensionless variables S, H/D, b_w/D, b_c/D, b_w/b_c and S_o. An output layer to represent the single output variable (the discharge). The hidden layer between the input and the output layer to receive the input, to perform the computations and to the send the outputs to the output layer. The hidden layer uses a transfer or activation function to modify the input to the neuron. The transfer function may be linear, sigmoid or tansh. Sigmoid or tansh are smooth nonlinear functions and one of them is normally chosen because the learning algorithm requires a response function with a continuous, single-valued first derivative. Building the MLP network is known as training.

The following steps summary the network training processes based on back-propagation learning algorithm, Neural Connection [12] and Negm [13].

i- The values of the weights are set to initial random values.
The normalized input pattern X_p (S, H/D, b_w/D, b_c/D, b_w/b_c and S_o) and the normalized target pattern T_p (Q) are shown to the network.

ii- The output (O) from each node in a layer is calculated. The output from a node j in the second layer is given by:

$$O_j = \phi\left(\sum_{i=1}^{n} w_{ij} x_i + b_j\right) \quad (7)$$

in which ϕ is the activation or transfer function of the node. The activation function in the present application is the hyperbolic tangent function (tansh) and b_j is the bias weight of the node j.

iii- The weights (w) between nodes are adjusted, starting from the output layer and working backwards. The new weight is given by:

$$w_{ij}(s+1) = w_{ij}(s) + \eta \delta_{pj} O_{pj} \quad (8)$$

in which $w_{ij}(s)$ is the weight between nodes i and j at step s before adjustment while $w_{ij}(s+1)$ is the same weight after adjustment, O_{pj} is the output value at node j, δ_{pj} is the error of pattern p at node j and η is the learning rate. The error δ_{pj} is given by

$$\delta_{pj} = O_{pj}\ (1 - O_{pj})(T_{pj} - O_{pj}) \quad (9)$$

iv- The steps from ii to iv are repeated until the error between the desired and the neural network output reaches a global minimum.

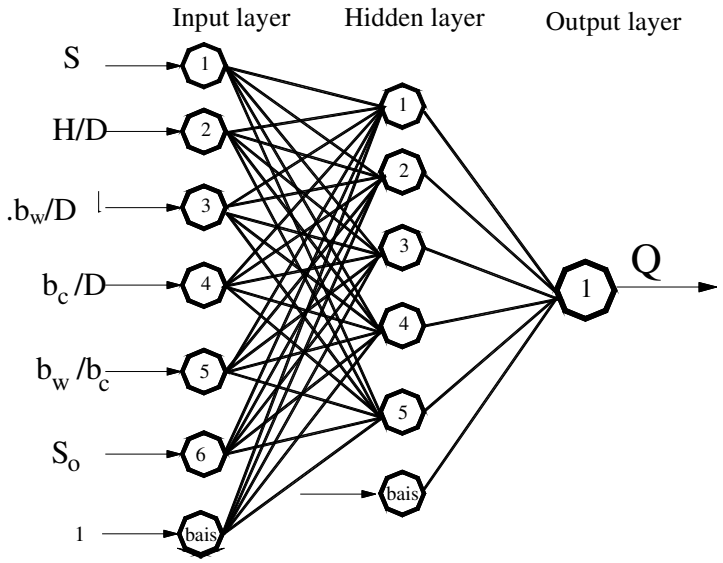

Figure 3 Topology of the developed ANN for the present application

6.1. TRAINING, VALIDATING AND TESTING THE ANN MODEL

The Neural Connection [12] is used to train the network of the present application. Several runs are performed using different values of the initial weights until optimal initial weights are obtained. In this application, the initial random weights are found to be within ± 0.02 generated using a seed of 7. The best activation function is found by trial and error to be the tansh. The application is run again with different number of neurons in the hidden layer. Many computer experiments are carried out using 1, 3, 6, 9, 12, 15, 20, 30, 50 and 100 neurons at the hidden layer. It is found that the best results are obtained at 6 neurons and no further improvement is obtained in the correlation coefficient between observed and predicted discharges. Similarly, the maximum number of iteration is found to be 500 (over a range of 10 to 10000 iterations). Further increase in the iterations shows no improvement till about 2500. Further increase more than 2500 increases the validation system error and decreases the training system error. An over-training occurs in this case and the network is called over-trained network which in turn lose the capability to generalize.

6.2. STABILITY OF THE NETWORK

Once the structure of the network is determined, its stability is studied. Several computer experiments are conducted using the pre-determined structure of the network but in each case the data sets are chosen randomly in different ways. The results of six experiments using different seeds of 5, 1, 3, 7, 2 & 10 are shown in Table 3. Experiment no. four show the best results, however, its results are not varying largely compared to other experiments.

Table 3 Results of network stability

Data set	Exp.1	Exp. 2	Exp. 3	Exp. 4	Exp. 5	Exp. 6
Training, R^2	0.996	0.996	0.996	**0.998**	0.997	0.997
Validation, R^2	0.997	0.997	0.998	**0.998**	0.998	0.996
Test, R^2	0.998	0.998	0.998	**0.998**	0.998	0.998

Figure 4 shows the prediction of the ANN model versus the measured discharges. Clearly, excellent agreement was obtained.

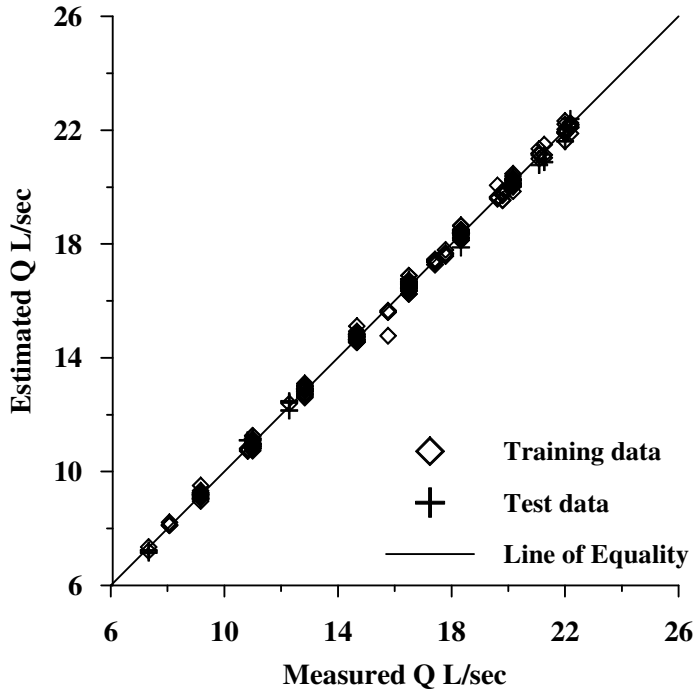

Figure 4. Prediction of ANN model versus the measured data for both training and test data sets

6.3. SENSITIVITY ANALYSIS

Sensitivity analysis is important in order to find the relative importance of the different dimensionless variables involved in the prediction model. Building the prediction model several times with one different dimensionless variable removed per time. Results of sensitivity analysis indicated that the importance of the variables is decreased in the following order, H/D, S, b_w/D, S_o, b_w/b_c and b_c/D. Table 4 presents the results of the sensitivity analysis. The percentage reduction in the correlation coefficient between the measured and the predicted values when a particular dimensionless variable is removed from the model is calculated. Clearly, the model is greatly affected when H/D is removed because the reduction in the correlation coefficient is the largest (12.02%), followed by the submergence ratio where a percentage reduction in R is 4.86%. Removing of other variables indicated less

reduction in R. This highlight the fact that the variables H/D and S should be determined very precisely to ensure reliable predictions.

Table 4 Results of sensitivity analysis

Data set	bc/D	bw/bc	So	bw/D	S	H/D
R	0.982	0.980	0.9745	0.9759	0.9380	0.8670
% reduction	0.460	0.530	0.680	1.050	4.860	12.020
Importance	6	5	4	3	2	1

7. ANN MODEL VERSUS OTHER MODELS

Figures 5a and 5b show the comparison among the prediction of the different models and the measured discharges. These figures indicate that the predictions due to ANN models are very close the line of equality, followed by the prediction to equation (5), then equation (2) and equation (1). This order is also clear from Table 2.

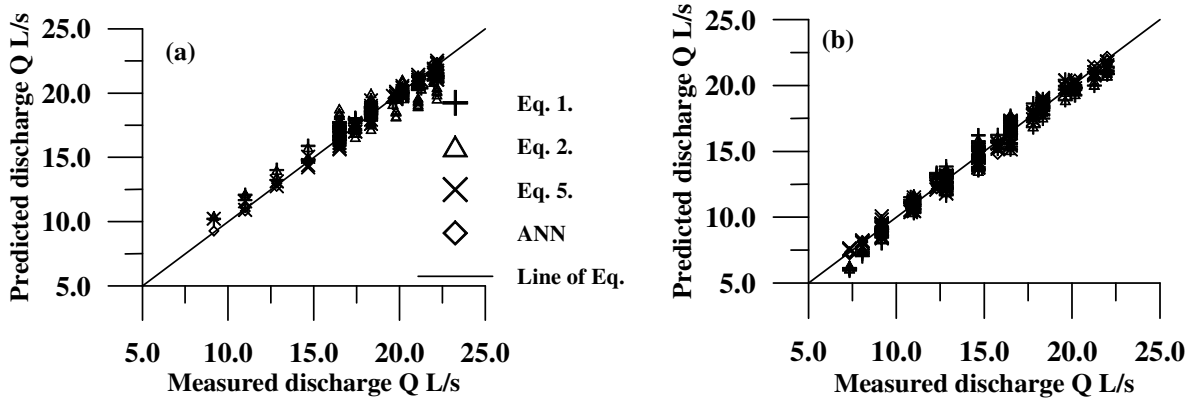

Figure 5. Comparison among predictions of different models using data from (a) Ref. [2] and (b) Ref. [1]

Figures 6a, 6b and 6c present the comparison among different models and the measured data for different submergence ratio S, different weir width ratio b_w/D and different culvert width ratio b_c/D respectively. These three sets were selected to represent the basic dimensionless ratios S, b_w/D and b_c/D affecting the flow through the structures. The data in the first two figures are due to Negm [2] and that in third figure are due to Mohamed [1]. Clearly, the above stated order is clear in these figures. These figures indicate that the results of the prediction models agreed generally well with the trend of the experimental data, where Q_{nd} ($Q_{nd} = Q/D^2\sqrt{2gD}$) increases with the increase of H/D, with the increase of S (Figure 6a), with the increase of b_w/D (Figure 6b) and with the increase of b_c/D (Figure 6c).

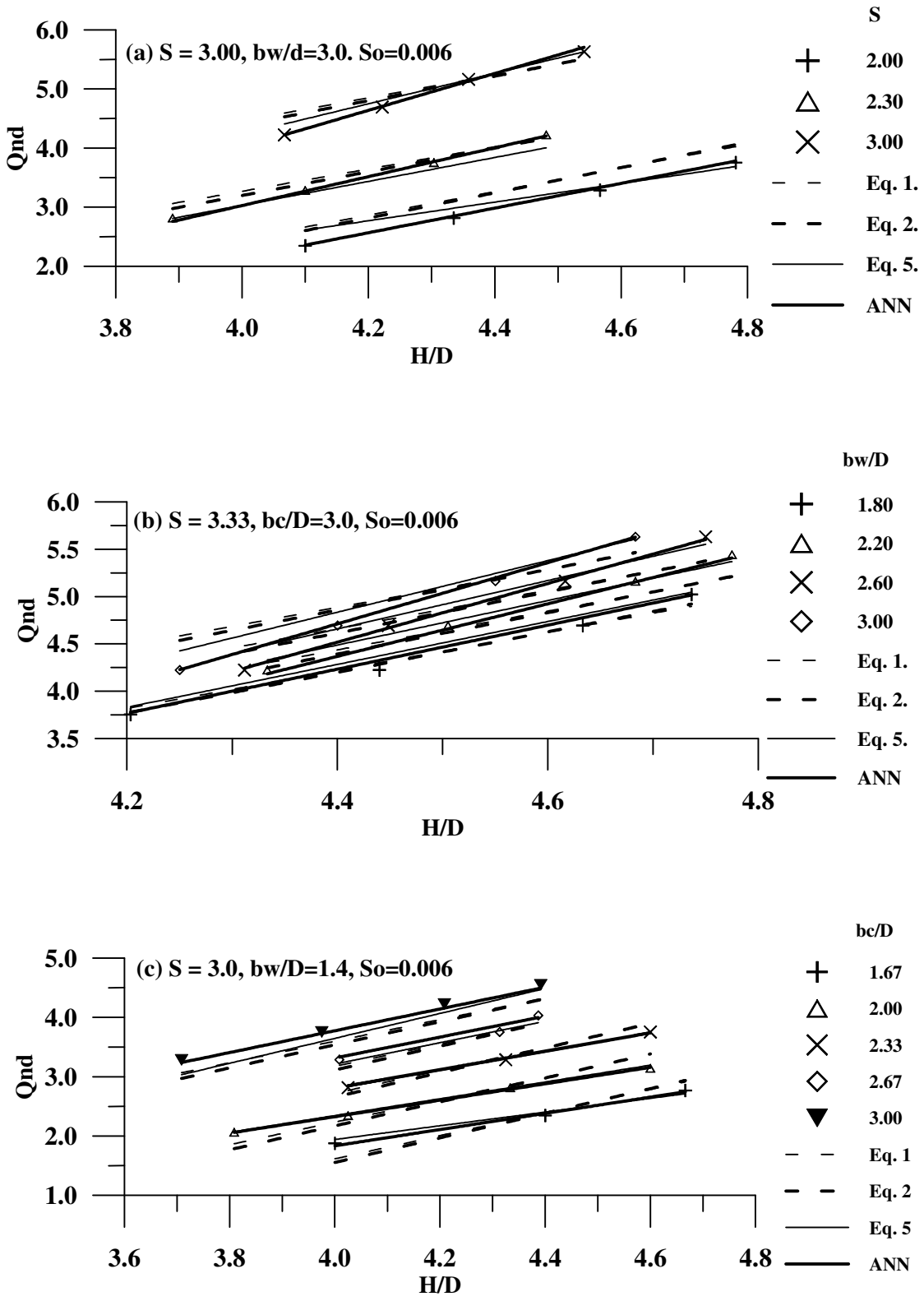

Figure 6. Typical comparisons among different prediction models and measured data for (a) different values of S, Ref. [2], (b) different values of b_w/D, Ref. [2], and (c) different values of b_c/D, Ref.[1].

8. CONCLUSIONS

The following main conclusions could be stated:

1- The proposed predicted model (equation 5) for computing the simultaneous discharge over BCW and through culvert (flow type 4) is much better than regression model (equations 1 and 2) and could be used for wide range of parameters provided equation 6 is re-built for the same range.
2- The predictions of the developed ANN model are much better than all other models including equation 5. In fact, most of the predicted values (about 98%) have errors less than 2.5%.
3- Sensitivity analysis indicated that the most important dimensionless variable is the relative upstream water depth H/D, followed by the submergence S, then b_w/D, S_o, b_w/b_c and finally b_c/D.

NOMENCLATURE

A_o cross sectional area of the culvert;
b_c width of the culvert vent;
b_j the bias weight of the node j;
b_w width of the weir;
B width of the channel;
C_w coefficient of discharge for weir;
C_D coefficient of discharge for culvert;
C_V coefficient of velocity;
D depth of culvert vent;
F simultaneous flow interaction factor;
G gravitational acceleration;
ht tailwater depth;
hw head over the weir;
H depth of water upstream the structure;
Hd depth of water just downstream the structure;
H_o total energy head;
L length of the culvert;
n Manning roughness coefficient;
Q combined discharge;
Q_c discharge through the culvert;
Q_{nd} non-dimension discharge ($Q_{nd} = Q/D^2\sqrt{2gD}$);
Q_w discharge over the weir;
R^2 determination coefficient;
R correlation coefficient;
R_o hydraulic radius;
P height of the weir;
T target;
O_{pj} output value at node j;
V_a velocity of approach;

S submergence;
S_o bottom slope;
$w_{ij}(s)$ weight between nodes i and j at step s before adjustment;
$w_{ij}(s+1)$ weight after adjustment;
δ_{pj} error of pattern p at node j;
η learning rate; and
ϕ activation or transfer function of the node.

ABBREVIATIONS

ANN = Artificial Neural Network
BCW = Broad-Crested Weir
Eq. = equation
Exp. = Experiment
MLP = Multi-Layer Perceptron
MRAE = Mean Relative Absolute Error
Ref. = Reference
RMSE= Root Mean Square Error
Tansh = Hyperbolic tangent function
PE = Processing Element
SEE = Standard Error of Estimate

REFERENCES

[1] Mohamed, M.S, "Characteristics and Prediction of Simultaneous Flow Over Broad-Crested Weirs and Through Culverts", Egyptian Journal for Engineering Science and Technology (EJEST), Faculty of Engineering, Zagazig University, Egypt. Vol. 6, No. 1, 2002, pp. 113-128.

[2] Negm, A.M., "Experimental Investigation on Simultaneous Flow through Combined Box Culverts and Over Contracted Broad-Crested Weirs", Proc. 2nd Int. Conf. for Advanced Trends in Engineering (MICATE'2002), April 7-9, Faculty of Engineering. Al-Minai University, Egypt, 2002b.

[3] Chow, V.T., "Open Channel Hydraulics", McGraw-Hill Int. Book Co., Tokyo. Japan, 1959.

[4] Herschy, R.W, (Editor), "Hydrometery", John Wile & Sons, New York, 1978.

[5] French R.H., "Open Channel Hydraulics", McGraw Hill Book Company, New York, 1985.

[6] Bodhaine, G.L., "Measurement of Peak Discharge at Culverts by Indirect Methods. U.S. Geological Survey", Techniques of Water Resources Investigations, Book 3, Chap. A3. Washington, 1976, First reprinted in 1968.

[7] Bos, M.G. (Editor), "Discharge Measurement Structures", Oxford & IBH Publishing Co., New Delhi, 1976.

[8] Negm, A.M., Alsheikh, A., "Characteristics of Flow Over Contracted Broad-Crested Weirs", Engineering Bulletin (Civil Engineering), Faculty of Engineering, Ain Shams University, Cairo. Egypt, Vol.32, No. 3, 1997, pp. 227-247.

[9] Grubert, J.P, "Application of Neural Networks in Stratified Flow: Stability Analysis", Journal Hydraulic Engineering, Vol. 121, No. 7, 1995, pp. 523-532 and Discussion, Vol. 123, No. 3, 1997, pp. 253-254.

[10] Dibike, Y.B. and Abbott, M.B., "Application of Artificial Neural Networks to the Simulation of a Two Dimensional Flow", Journal of Hydraulic Research, Vol. 37, No. 4, 1999, pp. 435-446.

[11] Dibike, Y.B., Minns, A.W. and Abbott, M.B., "Applications of Artificial Neural Networks to the Generation of Wave Equations From Hydraulic Data", Journal of Hydraulic Research, Vol. 37, No. 1, 1999, pp. 81-97 and Discussion in Vol. 38, No. 4, 2000, pp. 317-318.

[12] Neural Connections, "ANNs Software and User Manuals", SPSS Inc./Recognition Systems Inc, 1998.

[13] Negm, A.M., "Prediction of Hydraulic Design Parameters of Expanding Stilling Basins Using Artificial Neural Networks", Egyptian Journal of Engineering Science and Technology (EJEST), Vol. 6, No. 1, 2002a, pp. 1-24.